

Magnetic, magnetotransport, and optical properties of Al-doped Zn_{0.95}Co_{0.05}O thin films

M. Venkatesan,^{a)} P. Stamenov, L. S. Dorneles, R. D. Gunning, B. Bernoux, and J. M. D. Coey
CRANN and School of Physics, Trinity College, Dublin 2, Ireland

(Received 14 March 2007; accepted 21 May 2007; published online 14 June 2007)

Thin films of 5% Co-doped ZnO with a range of Al codoping exhibit a band-edge shift, which varies with carrier concentration as $n^{2/3}$. Carrier effective mass is $0.26m_e$ and mobility is $\sim 10 \text{ cm}^2 \text{ V}^{-1} \text{ s}^{-1}$. The doped films, which contain coherent Co clusters of 4–8 nm in size, exhibit a ferromagnetic moment of $0.3\text{--}1.0\mu_B$ per cobalt. The magnetism is progressively destroyed by Al doping due to a reduction in Co-cluster formation. Magnetoresistance appears below 30 K, but these materials cannot be regarded as dilute magnetic semiconductors. © 2007 American Institute of Physics.

[DOI: 10.1063/1.2748343]

There is an ongoing quest for ferromagnetic semiconductors with a Curie temperature well above room temperature, which could be used for the second generation of spin electronics, as well as a search for transparent ferromagnets which could add an optoelectronic dimension. An early report of room temperature ferromagnetism in ZnO was by Ueda *et al.*¹ in cobalt-doped thin films (Zn_{1-x}Co_x)O with $x=0.05\text{--}0.25$, which showed a large moment of $1.8\mu_B$ per cobalt ion for $x=0.05$. High-temperature ferromagnetism was subsequently found by other groups, with varying magnetic moments.^{2–6} A systematic variation of magnetic moment in transition metal doped ZnO films grown by pulsed laser deposition was found with 3d dopant.⁷

These reports have been received with skepticism, and the belief that the ferromagnetism must somehow be associated with clustering or incipient formation of a secondary ferromagnetic phase. Nevertheless, good spectroscopic evidence shows that the divalent cobalt does indeed substitute on the tetrahedral sites of the wurtzite structure.^{1,8–11} Searches by Rode *et al.*⁴ and Ramachandran *et al.*¹¹ revealed no evidence for phase segregation in Co-doped ZnO films, while close examination of other films has revealed the presence of cobalt nanoclusters in some cases.^{12,13}

ZnO has electron (n type) conductivity with appropriate dopants such as Al, Ga, etc. Heavy electron doping of up to $\sim 10^{21} \text{ cm}^{-3}$ can be realized in ZnO by using a proper doping technique. It is a challenge to achieve highly conducting Co:ZnO films without degrading their magnetic properties, as substitution of Co often leads to an increase in resistivity of films. A recent report correlated the magnetic moment and the carrier concentration in Co- and Mn-substituted films.¹⁴ From both the theoretical and experimental points of view, there are lots of open questions regarding the magnetism and magnetoresistance of these materials. Here, we report an investigation of magnetic, electrical, and optical properties of pure and Al codoped Zn_{0.95}Co_{0.05}O thin films, demonstrating the effect of Al on magnetic, transport, and optical properties of these transparent conducting oxide films.

Thin films [of pure and Al-doped (0.1 to 1 at. %) Zn_{0.95}Co_{0.05}O] were deposited at 450 °C, on both C-cut and R-cut sapphire substrates using the same conditions as reported earlier.⁷ Film thickness was monitored during deposi-

tion using optical reflectivity at 635 nm, and it was independently calibrated by small angle x-ray scattering. Thicknesses were in the range of 100–150 nm.

All films are highly oriented and x-ray diffraction patterns of films on C-cut and R-cut substrates showed (002) and (110) reflections of ZnO. Long scans with a multidetector revealed a small reflection at 44.3° (Cu K α), which is the (002) reflection of Co. Phi scans showed the cobalt to be coherent with the ZnO lattice. Using the Scherrer formula, we estimated the crystallite size as 4–8 nm, big enough to be blocked at room temperature.¹⁵

Magnetization measurements were made (in superconducting quantum interface device magneto-meter) by mounting the samples in straws after removing the corners of the $5 \times 5 \times 0.5 \text{ mm}^3$ substrates, with the field applied perpendicular to the substrate plane. The curve in Fig. 1(a) shows the diamagnetism of a blank Al₂O₃ substrate subjected to the same thermal cycle in the deposition chamber as one with a thin film deposited on it. The susceptibility of $-4.8 \times 10^{-9} \text{ m}^3 \text{ kg}^{-1}$ is in agreement with the accepted value. Figures 1(b) and 1(c) show the ferromagnetic signal of Co:ZnO film before and after subtracting the linear diamagnetic background signal arising from the substrate. Moments are quite variable, depending on the substrate, as shown in Table I. The observed moments per Co atom of doped films

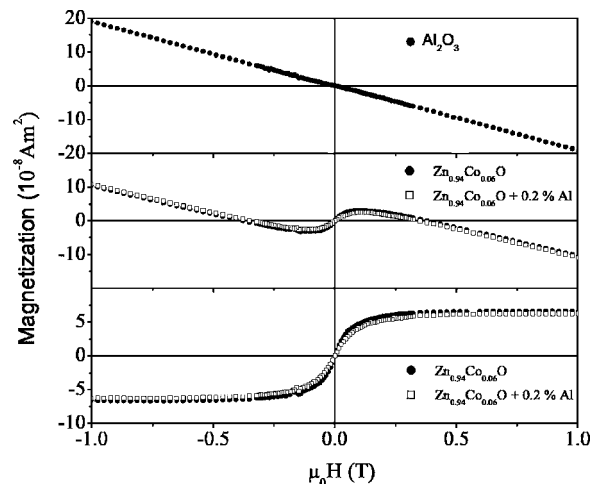


FIG. 1. Room temperature magnetization curves of (a) blank sapphire substrate and (b) Zn_{0.95}Co_{0.05}O and 0.2% Al-doped Zn_{0.95}Co_{0.05}O film, and (c) data after subtracting the diamagnetic contribution from the substrate.

^{a)}Electronic mail: venkatem@tcd.ie

TABLE I. Properties of pure and doped ZnO thin films grown on C- and R-cut sapphire substrates.

Composition	Substrate	σ (μ_B/Co)	E_g (eV)	ρ (Ω cm)	n (cm^{-3})
ZnO	C-Al ₂ O ₃	...	3.4	2.1×10^{-2}	8.1×10^{18}
	R-Al ₂ O ₃	...	3.4	...	2.2×10^{18}
Zn _{0.95} Co _{0.05} O	C-Al ₂ O ₃	1.0	3.4	1.5×10^{-4}	6.0×10^{17}
	R-Al ₂ O ₃	0.3	3.4
Zn _{0.95} Co _{0.05} O+0.1% Al ₂ O ₃	C-Al ₂ O ₃	0.5	3.5	3.5×10^{-3}	3.8×10^{19}
	R-Al ₂ O ₃	0.2	3.7
Zn _{0.95} Co _{0.05} O+0.2% Al ₂ O ₃	C-Al ₂ O ₃	0.6	3.7	7.4×10^{-5}	2.3×10^{20}
	R-Al ₂ O ₃	0.1	3.8	...	1.4×10^{20}
Zn _{0.95} Co _{0.05} O+0.5% Al ₂ O ₃	C-Al ₂ O ₃	0.4	4.0	2.3×10^{-5}	3.3×10^{20}
	R-Al ₂ O ₃	0.06	3.9
Zn _{0.95} Co _{0.05} O+0.7% Al ₂ O ₃	C-Al ₂ O ₃	0.4	4.1	1.7×10^{-5}	3.6×10^{20}
	R-Al ₂ O ₃	0.05	4.0
Zn _{0.95} Co _{0.05} O+1.0% Al ₂ O ₃	C-Al ₂ O ₃	0.07	4.1	1.5×10^{-5}	3.6×10^{20}
	R-Al ₂ O ₃	0.06	4.1

on C-cut sapphire substrates are always greater than on R-cut substrates, as shown in Fig. 2. Films with no Al exhibit a low temperature magnetization that can be interpreted in terms of a paramagnetic component (saturating at low temperature and high field) that is attributed to substitutional Co²⁺, as well as the ferromagnetic component showing a temperature-activated decrease of coercivity which is attributed to the Co metal clusters. The mean cluster size evaluated from the activation energy using the bulk anisotropy constant of cobalt is 8 nm, in reasonable agreement with diffraction data on the same samples.

The Co/ZnO atomic ratio in the films can be roughly estimated from the area under the peaks, obtained from x-ray diffraction measurements, as the intensity of a given reflection I_{hkl} is proportional to $[F_{hkl}/\sin \theta]^2$, where F_{hkl} is the structure factor. From that ratio, an estimate of the saturation magnetic moment due to metallic Co is similar to that of the measured magnetic moment. The striking point is that the magnetic moment we observe is proportional to the amount of metallic Co present in the film, which decreases with Al doping. This is quite different from the room temperature ferromagnetism observed in high-temperature grown films reported earlier.⁷

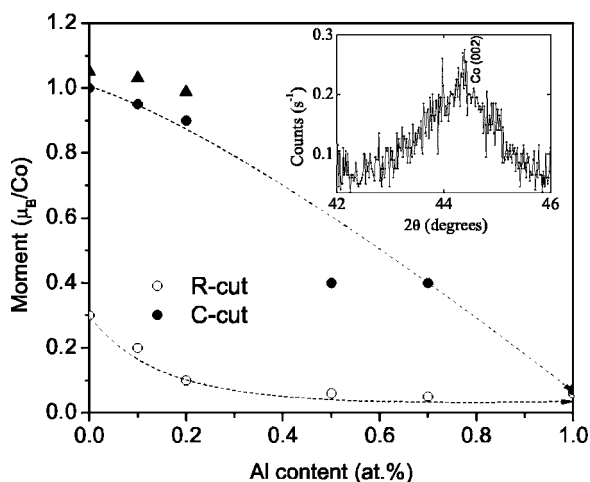


FIG. 2. Magnetic moment of Zn_{0.95}Co_{0.05}O films as a function of Al content on R-cut (○) and C-cut (●) sapphire substrates. ▲ denotes the saturation magnetic moment estimated from the x-ray diffraction measurements. Estimated error is $\pm 50\%$. The inset shows the (002) reflection from metallic Co.

Transport measurements, in the temperature interval of 2–300 K, were performed on samples contacted by shadow masking and thermal evaporation of Al/Au bilayer at pressures below 10^{-6} mbar. The conductivity of 5% Co-doped ZnO is modified by Al doping.

Magnetoresistance and Hall resistance were extracted by symmetrizing and antisymmetrizing with respect to field the R_{xy} measured in the van der Pauw geometry. Samples exhibit appreciable magnetoresistance only below about 30 K, with a strong temperature dependence governed by both carrier concentration and mobility. There is no measurable anomalous Hall effect. The magnetoresistance at 2 K is plotted on Fig. 3(a), where it reaches about 5.5%. These data can be qualitatively understood in terms of a superposition of standard open- and closed-orbit magnetoresistance, ionized impurity magnetoresistance,¹⁶ and weak localization magnetoresistance.¹⁷ The carrier concentration deduced from the Hall effect has a nonlinear dependence on Al concentration [see inset in Fig. 3(b)] and shows saturation at about 0.2% Al, evidence for either a low solubility limit for the Al or complete degeneracy of the electron gas at $n > 2 \times 10^{20} \text{ cm}^{-3}$. Mobilities are found to be in the region of 0.4–11.4 $\text{cm}^2 \text{ V}^{-1} \text{ s}^{-1}$ at 2 K. The temperature dependence of the Hall resistance shown on Fig. 3(b) reveals almost degenerate electronic concentrations even without Al doping, and virtually no temperature dependence for the films with more than 0.2% Al. The magnetoresistance generally diminishes with increased carrier concentration, with the exception of the 0.2% Al film, shrinking to essentially zero for more than 0.5% Al, which is further evidence for the degeneracy of the electron gas in the high doping regime. The detailed analysis of the magnetoresistance is complicated by the possible dimensional crossover from three-dimensional weak localization where the correction to the resistivity is of the order $2\pi^2\hbar\sqrt{e/\hbar B}/e^2$, at fields above 1 T for film thickness $t=80$ nm to a thickness-limited two-dimensional localization where the correction to the resistivity is of the order $\pi\hbar t/e^2$. This is likely the reason why the magnitude of the magnetoresistance for all samples except the one with 0.2% Al does not decrease for fields beyond about 3 T. The positive initial magnetoresistance for 0.2% Al is likely due to a closed orbit on the Fermi surface becoming accessible at filling corresponding to conduction electron concentrations of about $4 \times 10^{20} \text{ cm}^{-3}$.

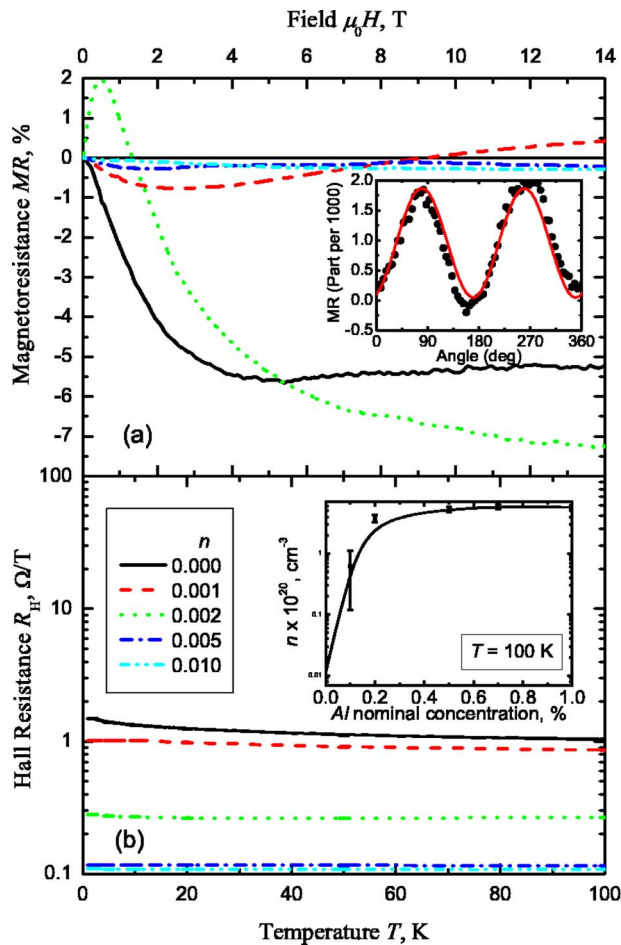


FIG. 3. (Color online) (a) Magnetoresistance measured at 2 K for various nominal Al concentrations. The inset shows the anisotropy of the magnetoresistance for 0.2% Al measured in field of 14 T at 2 K. (b) Hall resistance as a function of temperature for the same compositions. The inset illustrates the complete degeneration of the electronic gas at 0.2% Al.

Samples with less than 0.2% Al exhibit substantial anisotropy of the in-plane magnetoresistance. The effect can be as large as 19% at 2 K for some samples without Al doping. The observed angular dependence can be fitted with up to three terms varying for $n=1, 2, 3$ as $A_n \sin^{2n}(\theta - \phi)$, where θ is the angle between the field and current vectors, ϕ is an offset angle which depends on the crystallographic orientation, and A_n are amplitude factors. An example for 0.2% Al, measured at field of 14 T and temperature of 2 K is shown as inset in Fig. 3. The observed effect is attributed to the anisotropy of the Fermi surface and not to conventional AMR.

Optical transmission spectra for Al-doped Co:ZnO thin films are presented in Fig. 4. The Al doping leads to band-gap widening. The band gap increases from 3.7 eV (no Al) to 4.5 eV (1 at. % Al), as a result of filling of the lowest states in the conduction band by Al donor electrons—the Burstein-Moss effect.¹⁸ The expected functional dependence of the shift for a free-electron conduction band, $\Delta E_g = (\hbar^2/2m^*) \times (3\pi^2 n_e)^{2/3}$,¹⁹ is well satisfied, within experimental error, and yields a mean harmonic mass defined by $1/m^* = 1/m_e + 1/m_h$ with $m^* = 0.26(3)m_e$, which is in good agreement with the accepted values of $m_e = 0.23$ and $m_h = 0.59$ for Al-doped ZnO.²⁰

In conclusion, we find no intrinsic relation between magnetization and electron concentration in our Al-doped $(\text{Zn}_{0.95}\text{Co}_{0.05})\text{O}$ films. The disappearance of magnetism with

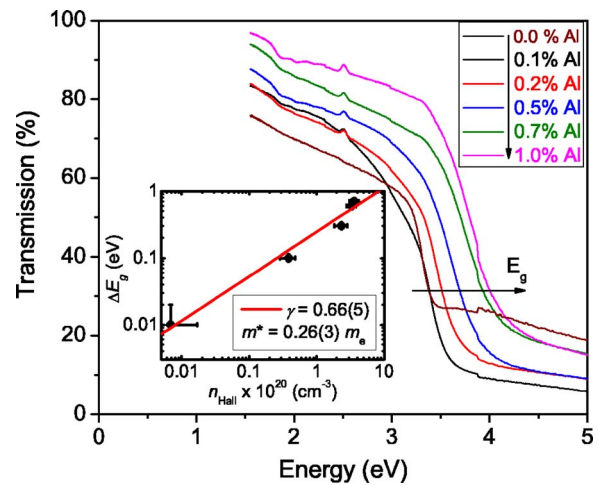


FIG. 4. (Color online) Room temperature optical spectra of Co:ZnO films at different Al concentrations. The inset shows reduced data on the band-gap shift due to the Burstein-Moss effect and a fit to it revealing correct power law behavior with $\gamma = 2/3$.

Al doping is related to the disappearance of cobalt nanoclusters. Interesting magnetoresistance is observed below 30 K, but neither it nor the absence of an anomalous Hall effect supports the idea that these materials are dilute magnetic semiconductors.

This work was supported by the Science Foundation of Ireland, as part of the MANSE project. L. S. Dorneles is supported by the Irish Research Council for Science, Engineering and Technology.

- ¹K. Ueda, H. Tabata, and T. Kawai, *Appl. Phys. Lett.* **79**, 988 (2001).
- ²Y. M. Cho, W. K. Choo, H. Kim, D. Kim, and Y. E. Ihm, *Appl. Phys. Lett.* **80**, 3358 (2001).
- ³H. J. Lee, S. Y. Jeong, C. R. Cho, and C. H. Park, *Appl. Phys. Lett.* **81**, 4020 (2002).
- ⁴K. Rode, A. Anane, R. Mattana, J. P. Contour, O. Durand, and R. LeBourgeois, *J. Appl. Phys.* **93**, 7676 (2003).
- ⁵W. Prellier, A. Fouchet, B. Mercey, C. Simon, and B. Raveau, *Appl. Phys. Lett.* **82**, 3490 (2003).
- ⁶D. P. Norton, M. E. Overberg, S. J. Pearton, K. Pruessner, J. D. Budai, L. A. Boatner, M. F. Chisholm, J. S. Lee, Z. G. Khim, Y. D. Park, and R. G. Wilson, *Appl. Phys. Lett.* **83**, 5488 (2003).
- ⁷M. Venkatesan, C. B. Fitzgerald, J. G. Lunney, and J. M. D. Coey, *Phys. Rev. Lett.* **93**, 177206 (2004).
- ⁸K. Ando, H. Saito, Z.-W. Jin, T. Fukumura, M. Kawasaki, Y. Matsumoto, and H. Koinuma, *Appl. Phys. Lett.* **78**, 2700 (2001).
- ⁹K. J. Kim and Y. R. Park, *Appl. Phys. Lett.* **81**, 1420 (2001).
- ¹⁰D. A. Schwartz, N. S. Norberg, Q. P. Nguyen, J. M. Parker, and D. M. Gamelin, *J. Am. Chem. Soc.* **125**, 13205 (2003).
- ¹¹S. Ramachandran, A. Tiwari, and J. Narayan, *Appl. Phys. Lett.* **84**, 5255 (2004).
- ¹²J. H. Park, M. G. Kim, H. M. Jang, S. Rhu, and Y. M. Kim, *J. Appl. Phys.* **84**, 1338 (2004).
- ¹³L. S. Dorneles, M. Venkatesan, R. Gunning, P. Stamenov, J. Alaria, M. Rooney, J. G. Lunney, and J. M. D. Coey, *J. Magn. Magn. Mater.* **310**, 2087 (2007).
- ¹⁴X. H. Hu, H. J. Blythe, M. Ziese, A. J. Behan, J. R. Neal, A. Mokhtari, R. M. Ibrahim, A. M. Fox, and G. A. Gehring, *New J. Phys.* **8**, 135 (2006).
- ¹⁵J. C. Denardin, M. Knobel, L. S. Dorneles, and L. F. Schelp, *J. Magn. Magn. Mater.* **294**, 206 (2005).
- ¹⁶P. Stamenov, M. Venkatesan, L. S. Dorneles, D. Maude, and J. M. D. Coey, *J. Appl. Phys.* **99**, 08M142 (2006).
- ¹⁷T. Andrearczyk, J. Jaroszynski, G. Grabecki, T. Dietl, T. Fukumura, and M. Kawasaki, *Phys. Rev. B* **72**, 121309R (2005).
- ¹⁸E. Burstein, *Phys. Rev.* **93**, 632 (1954); T. S. Moss, *Proc. Phys. Soc. London, Sect. B* **67**, 775 (1954).
- ¹⁹I. Hamberg and C. G. Granqvist, *Phys. Rev. B* **30**, 3240 (1984).
- ²⁰B. E. Semelius, K. F. Berggren, Z. C. Jin, I. Hamberg, and C. G. Granqvist, *Phys. Rev. B* **37**, 10244 (1988).